High Resolution Range Imaging via Model-based Compressed Sensing

V. Adler[1], **J. Moll**[2], **M. Kuhnt**[2], **B. Hils**[2], **V. Krozer**[2], **and K. Hoffmann**[1]

[1]Department of Electromagnetic Field, Faculty of Electrical Engineering, CTU in Prague, Czech Republic
[2]Department of Physics, Goethe University Frankfurt am Main, Frankfurt am Main, Germany

Abstract— The paper proposes a method for high resolution range imaging at millimeter wave frequencies (85 GHz to 100 GHz) based on model-based compressed sensing (CS). A detailed description of the underlying CS-theory, the experimental setup and radar sensor are presented along with experimental results for one-dimensional range imaging. The proposed method is based on motorized reference measurements, which form the dictionary matrix for subsequent CS-processing. These reference measurements are tested against measurements from a glass fiber reinforced polymer (GFRP) component. A comparison of the CS-processed data to a classical Fourier-domain analysis revealed superior ranging performance of the CS-approach at the expense of a higher signal processing load.

1. INTRODUCTION

Compressed Sensing (CS) is an exciting radar based signal processing which reduces data rates by solving an underdetermined system of linear equations and has the potential to increase the range resolution of the radar range profiles which may be conducive to improved object detection and localization capabilities. Recent advances of compressed sensing applied to radar can be found, for example, in [1, 2].

This paper presents a case study of the CS-formulation in [3] for complex-valued signals where experiments are to be performed using a radar-transceiver in the mm-wave frequency range. The paper is organized in the following way: Section 2 presents the theoretical background of the CS-formulation and the experimental setup and the signal processing results are presented in Sections 3 and 4, respectively.

2. THEORETICAL BACKGROUND

2.1. Basics of Compressed Sensing

Herewithin is a short overview concerning current CS-based strategies for complex-valued signals. Consider the complex scene $\mathbf{b} \in \mathbb{C}^n$. To obtain information about the scene, m measurements are recorded. The measurement process is described as

$$\mathbf{y} = \mathbf{\Phi b} + \mathbf{e}, \tag{1}$$

in which $\mathbf{y} \in \mathbb{C}^m$ denotes the measurements, $\mathbf{\Phi} \in \mathbb{C}^{m \times n}$ models the linear measurement process and $\mathbf{e}$ is the measurement noise. Assuming that the number of measurements m is much smaller than the dimension of the signal n, Equation (1) becomes underdetermined. Nevertheless, in the CS-theory scene $\mathbf{b}$ can still be recovered if there is an orthonormal basis $\mathbf{\Psi} \in \mathbb{C}^{n \times n}$, so that $\mathbf{b} = \mathbf{\Psi x}$, in which $\mathbf{x} \in \mathbb{C}^n$ denotes a sparse vector.

One of the most prominent reconstruction techniques is Basis Pursuit Denoising (BPDN) [4]. The principle of BPDN is the solution of the following problem:

$$\min_x \frac{1}{2} \|\mathbf{y} - \mathbf{Ax}\|_2 + \lambda \|\mathbf{x}\|_1, \tag{2}$$

where $\mathbf{A}$ is the dictionary matrix $\mathbf{A} = \mathbf{\Phi\Psi}$ and λ represents a regularization parameter enforcing the sparsity of $\mathbf{x}$.

Most contemporary algorithms solving this problem can only be applied to real-valued signals. Thus, the complex signals have to be decoupled as follows:

$$\tilde{A} = \begin{pmatrix} \Re\{\mathbf{A}\} & -\Im\{\mathbf{A}\} \\ \Im\{\mathbf{A}\} & \Re\{\mathbf{A}\} \end{pmatrix}, \tag{3}$$

$$\tilde{\mathbf{y}} = \begin{pmatrix} \Re\{\mathbf{y}\} \\ \Im\{\mathbf{y}\} \end{pmatrix}, \tag{4}$$

and

$$\tilde{\mathbf{x}} = \begin{pmatrix} \Re\{\mathbf{x}\} \\ \Im\{\mathbf{x}\} \end{pmatrix}, \tag{5}$$

where $\Re\{\cdot\}$ and $\Im\{\cdot\}$ are the real and imaginary parts, respectively. These decomposed signals can then be treated with common CS-solvers like SPGL1 and TFOCS (see [5–7]).

2.2. Compressed Sensing Applied to IQ-modulated Signals

Consider a multistatic radar setup with N_{Tx} transmitters and N_{Rx} receivers using inphase and quadrature (IQ) demodulation. To obtain information on the radar scene $\mathbf{b} \in \mathbb{C}^n$ m measurements are recorded. Assuming that the number of scatterers N_S is small, the measurement process is represented as

$$\mathbf{y} = \mathbf{A}\mathbf{x} + \mathbf{e}, \tag{6}$$

where x is the image vector containing only N_S non-zero entries and $\mathbf{A}$ is the dictionary matrix. The additive noise term is again denoted as $\mathbf{e}$. Consider measurements from a single transmitter-receiver pair m; then the IQ-signal $\mathbf{y_m} = I_m(t) + jQ_m(t)$ can be represented as

$$\mathbf{y_m} = \mathbf{A_m}\mathbf{x_m} + \eta \tag{7}$$

where non-zero entries correspond to scatterers and $\mathbf{A_m} = [\mathbf{y}_{1m}^{model}, \mathbf{y}_{2m}^{model}, \cdots, \mathbf{y}_{Nm}^{model}]$ is the dictionary comprising the scattered signals, with $\mathbf{y}_{nm}^{model}$ corresponding to the expected signal for a scatterer located at distance x_n for the transmitter-receiver pair m.

As there are a total number of $p = N_{Tx} \times N_{Rx}$ pairs of transducers, we obtain the following system of equations

$$\mathbf{y_1} = \mathbf{A_1}\mathbf{x_1} + \eta, \tag{8}$$
$$\mathbf{y_2} = \mathbf{A_2}\mathbf{x_2} + \eta, \tag{9}$$
$$\vdots \tag{10}$$
$$\mathbf{y_m} = \mathbf{A_m}\mathbf{x_m} + \eta. \tag{11}$$

By concatenating these vectors and solving this equation using a common CS-solver, we can then determine the distance between the target and each transmitter-receiver pair.

3. EXPERIMENTAL SETUP

The measurement setup consists of a fully coherent stepped frequency continuous wave (SFCW) radar sensor, where the schematic of the sensor is shown in Fig. 1(a). To have a more flexible and rearrangeable measurement system working in the W frequency band the waveguide implementation of all main components, as depicted in Fig. 1(b), was chosen. A frequency multiplication (x6) of the output signal with a maximum frequency of 18 GHz was used and to ensure a high dynamic range of the measurement system power levels were optimized so the receiver in the TEST channel always worked in linear mode. Moreover, both receivers in the REF. and TEST path had significant reflections on its input ports so that a strong frequency dependence was observed in the path from directional coupler outputs to the receivers inputs. Consequently, a lock-in amplifier was used as the IQ demodulator because of its high dynamic range capabilities. The only disadvantage of using the proposed lock-in amplifier was the relatively long time of 0.5 s to lock on to the IF of 10 MHz at each new frequency point of the frequency sweep. To avoid time instabilities and excessively high phase noise in the IF signal, both RF and LO synthesizers were coupled with a single 10 MHz frequency standard. The employed antennas were a custom-made horn antenna with a gain of approx. 14 dB.

To exploit the dynamic range of the measurement setup maximally the device under test (DUT) had to be sufficiently large with respect to the antenna beamwidth and the distance from the antenna to achieve the aim of receiving most of the reflected wave from the DUT. The CS technique requires round-trip calibration measurements that form the dictionary matrix. To study the performance of the CS technique the reference positions of the DUT had to be very dense. Hence, manual positioning of the DUT was unacceptable, so a motorized linear stage which provided positioning

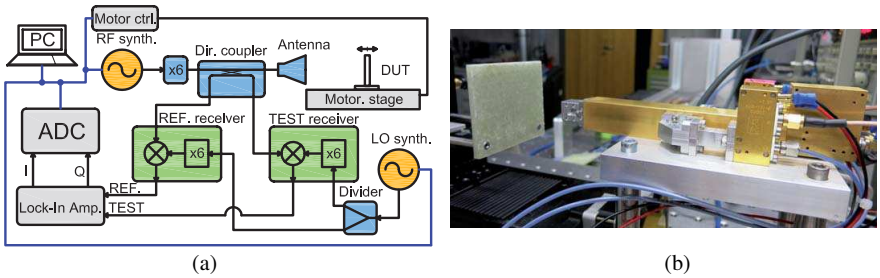

Figure 1: (a) Schematic of the radar sensor, (b) photo of the experimental setup.

precision better than 1 µm was used. The whole measurement setup was connected via GPIB and RS-232 databus and controlled from a computer using custom-made application programmed in Matlab resulting in completely automated measurement setup.

The dictionary was then designed using experimentally determined IQ-signals incorporating the complex envelope $y = I + jQ$. The SPGL1 method, considered to be one of the best available solvers [8] was used for signal reconstruction, and these results were compared with the TFOCS solver using Lan, Lu and Monteiro's accelerated method which restarts every 200 iterations [5, 9].

4. RESULTS

A total of 3,501 measurements covering an interval of 10 mm were recorded. In these measurements a flat aluminum plate was used as a reference reflector that had been translated linearly using a motorized stage. The spacing between two adjacent measurements was, hence, approximately 3 µm. To ensure the stable operation of the two synthesizers and the Lock-In amplifier the total time for data acquisition in this case study was around 1.5 days. The frequency range of the measurements was 85 GHz to 100 GHz using 51 frequency points. In total 500 measurements per frequency point were recorded and averaged to increase the signal-to-noise ratio. Moreover, an open-measurement was measured by placing an attenuator before the DUT to eliminate the reflections inside the antenna by simple subtraction. In the subsequent step, eleven test measurements from a glass-fiber-reinforced structure were recorded as shown in Fig. 1(b).

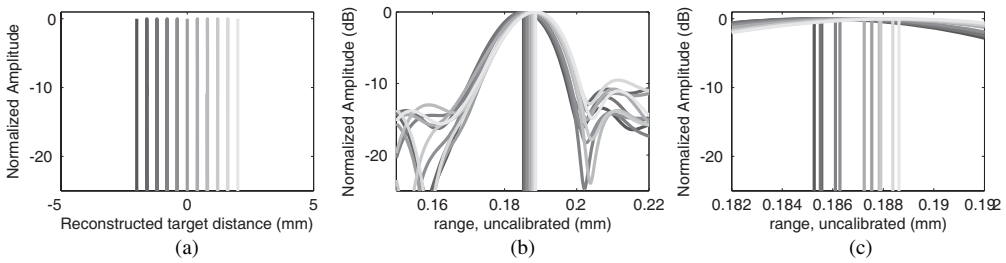

Figure 2: (a) Reconstructed high resolution range profiles using the proposed CS-approach, (b) conventional Fourier transform to create the range profiles, (c) close-up of the range profiles shown in (middle), where the spike train indicates the maximum values.

Figure 2 compares the range profile from conventional Fourier-domain radar signal processing with the range profiles obtained by the proposed CS-method. Fig. 2(a) shows that the CS-processed range profiles exhibit a very high resolution (spike train) for each considered measurement position in the interval $[-2, 2]$. In contrast, the conventional FFT-based range profiles strongly overlap and the localization error, represented by the position of the maximum, changes non-uniformly as shown in Figs. 2(b), 2(c). This result proves that the CS-framework enables very precise range imaging with excellent accuracy determined by the spacing of the reference measurements that constitute the dictionary. At the same time the proposed CS-approach demonstrates robustness against additional random measurement noise.

Figure 3 shows the effect when the dictionary does not cover the actual position of the current measurement. This directly leads to the off-grid case which aims to reconstruct the target at a position that is not covered by the dictionary measurements. Therefore, Fig. 3(a), firstly, shows the basis pursuit solution implemented in TFOCS. It can be observed that a single target can

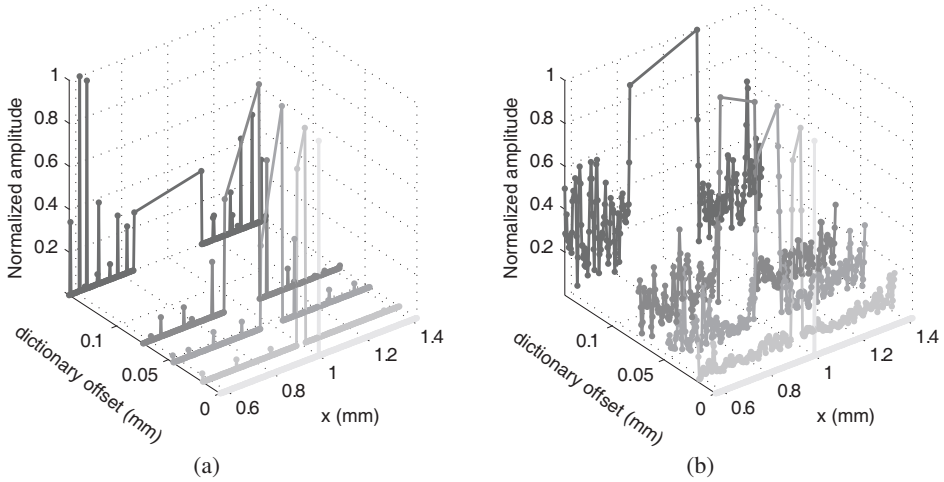

Figure 3: Analysis of the off-grid effect: Reconstruction errors occur when increasing the distance offset to the target in the dictionary for (a) the basis pursuit (implemented in TFOCS) and (b) basis pursuit denoise problem (implemented in the SPGL1 software package). The actual target position in this example is $x = 1\,\mathrm{mm}$.

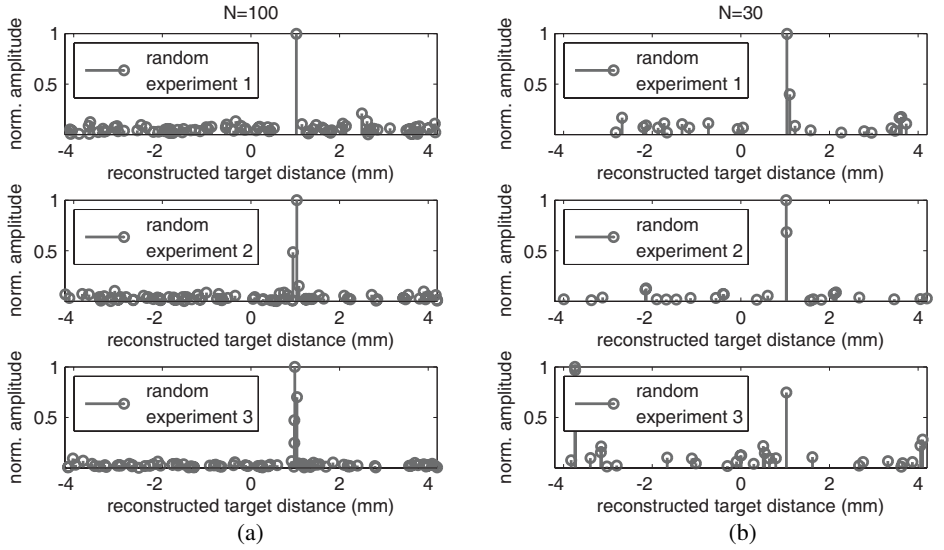

Figure 4: Effect of non-equidistant sampling based on uniform distribution for random dictionary selection and basis pursuit denoise problem: (a) three random experiments using $N = 100$ measurement positions (from a total of 3,501 measurements), (b) three random experiments using a subset of $N = 30$ measurement positions..

be accurately reconstructed when the dictionary offset tends to zero. When the dictionary offset increases the corresponding signal energy is split to the adjacent measurements points. Due to a large dictionary offset several spurious peaks occurred leading to erroneous results. Slightly different results have been obtained by the solution of the basis pursuit denoising problem implemented in the SPGL1 software package. Although the same scenario has been considered, the erroneous peaks had a lower amplitude, but the energy of the intended peak has been separated to the adjacent measurement points.

The conventional Fourier-domain signal processing produces range profiles by multiplying the time-domain signal with the speed of light. This results in an equidistant sampling of the signal which is not necessarily required in the proposed CS-approach as shown in Fig. 4. Here, two scenarios with a different number of sampling points are considered, i.e., $N = 100$ and $N = 30$. In each case three random experiments have been conducted to take the respective number of sampling points from a uniform distribution. It can be concluded that the position of the target which is located in this example at $x = 1\,\mathrm{mm}$ can be correctly reconstructed for 100 sampling points. On the other hand, when the number of sampling points is further reduced, it is then likely that spurious

peaks occur at incorrect positions. However, this result demonstrated the possibility of having a reduction of sampling points which is beneficial for various applications.

5. CONCLUSION

In this paper it was demonstrated that Compressed Sensing can be used to perform accurate Time-of-flight measurements taking into account complex valued measurement data as the dictionary. The limitations of the proposed approach were demonstrated in terms of the varied number of non-equidistant sampling points as well as the off-grid effects. Concerning the off-grid effect, it was found that solving the basis pursuit and the basis pursuit denoising problem leads to spurious signal components that degrade the ranging result.

ACKNOWLEDGMENT

This research was supported by the German Aerospace Center under grant number: 50RA1326 and by the Student Grant Competition under program SGS13/198/OHK3/3T/13 of the Czech Technical University in Prague.

REFERENCES

1. Ender, J. H., "On compressive sensing applied to radar," *Signal Processing, Special Section on Statistical Signal & Array Processing*, Vol. 90, No. 5, 1402–1414, 2010.
2. Cetin, M., I. Stojanovic, N. Nhon, K. Varshney, S. Samadi, W. Karl, and A. Willsky, "Sparsity-driven synthetic aperture radar imaging: Reconstruction, autofocusing, moving targets, and compressed sensing," *Signal Processing Magazine, IEEE*, Vol. 31, No. 4, 27–40, Jul. 2014.
3. Kuhnt, M., J. Moll, and V. Krozer, "A compressed sensing formulation based on i/qdictionary: experimental case study at millimeter-wave frequencies," *9th German Microwave Conference (GeMiC 2015)*, 229–232, 2015.
4. Chen, S. S., D. L. Donoho, and M. A. Saunders, "Atomic decomposition by basis pursuit," *SIAM Review*, Vol. 43, No. 1, 129–159, 2001, [Online] Available: http://dx.doi.org/10.1137/S003614450037906X.
5. Becker, S., E. Candés, and M. Grant, "Templates for convex cone problems with applications to sparse signal recovery," *Mathematical Programming Computation*, Vol. 3, No. 3, 165–218, 2011.
6. Van den Berg, E. and M. P. Friedlander, "Probing the pareto frontier for basis pursuit solutions," *SIAM Journal on Scientific Computing*, Vol. 31, No. 2, 890–912, 2008, Available: http://link.aip.org/link/?SCE/31/890.
7. Van den Berg, E. and M. P. Friedlander, "SPGL1: A solver for large-scale sparse reconstruction," June 2007, http://www.cs.ubc.ca/labs/scl/spgl1.
8. Van den Berg, E. and M. P. Friedlander, "Probing the pareto frontier for basis pursuit solutions," *SIAM Journal on Scientific Computing*, Vol. 31, No. 2, 890–912, 2009, [Online] Available: http://dx.doi.org/10.1137/080714488.
9. Becker, S., E. Candés, and M. Grant, "Templates for first-order conic solvers user guide," [Online] Available: http://cvxr.com/tfocs/doc/.